A Method to Study Precision Grip Control in Viscoelastic Force Fields Using a Robotic Gripper

Olivier Lambercy, *Member, IEEE*, Jean-Claude Metzger, *Student Member, IEEE*, Marco Santello, *Member, IEEE*, and Roger Gassert*, *Senior Member, IEEE*

***Abstract*—Instrumented objects and multipurpose haptic displays have commonly been used to investigate sensorimotor control of grasping and manipulation. A major limitation of these devices, however, is the extent to which the experimenter can vary the interaction dynamics to fully probe sensorimotor control mechanisms. We propose a novel method to study precision grip control using a grounded robotic gripper with two moving, mechanically coupled finger pads instrumented with force sensors. The device is capable of stably rendering virtual mechanical properties with a wide dynamic range of achievable impedances. Eight viscoelastic force fields with different combinations of stiffness and damping parameters were implemented, and tested on eight healthy subjects performing 30 consecutive repetitions of a grasp, hold, and release task with time and position constraints. Rates of thumb and finger force were found to be highly correlated ($r > 0.9$) during grasping, revealing that, despite the mechanical coupling of the two finger pads, subjects performed grasping movements in a physiological fashion. Subjects quickly adapted to the virtual dynamics (within seven trials), but, depending on the presented force field condition, used different control strategies to correctly perform the task. The proof of principle presented in this paper underscores the potential of such a one-degree-of-freedom robotic gripper to study neural control of grasping, and to provide novel insights on sensorimotor control mechanisms.**

***Index Terms*—Damping, haptic interface, mechanical impedance, sensorimotor memory, stiffness, virtual dynamics.**

I. Introduction

GRASPING objects with unfamiliar mechanical properties and generating appropriate forces for stable manipulation are tasks that rely on a complex interplay between prediction of sensory feedback arising from the hand–object interaction and afferent signals from the hand [1]–[3]. Sensory predictions can be defined as an internal representation of the mechanical properties of the object to be manipulated. Sensory predictions are based on an estimation (e.g., from visual inspection) and/or implicit knowledge from prior interactions, i.e., sensorimotor memory [3]–[5]. For example, it has been shown that humans form internal representations of the weight, texture, mass distribution, and compliance of manipulated objects in order to apply appropriate interaction forces [6]–[10]. The neural mechanisms underlying the formation of such models and how humans learn to adapt their grasp to objects of unknown or dynamically varying mechanical properties are areas of active investigation.

While most studies on grasp control focused on interaction with rigid objects, the grasping of compliant objects with viscoelastic properties (i.e., a combination of stiffness and damping, as encountered in many everyday objects such as a sponge, a pillow or a plastic cup) is a more complex sensorimotor task, as both finger position and fingertip force need to be simultaneously and continuously modulated. One approach to studying how humans control grasping of elastic loads is to use instrumented objects combining force/torque sensors and passive mechanical elements. Several groups have developed instrumented passive mechanisms with springs of different stiffness to challenge grip stability and evaluate the role of afferent feedback in the control of finger force and position [9], [11]–[13]. However, a major limitation of instrumented objects and passive mechanisms lies in the limited diversity of object properties that can be experimentally tested. Furthermore, changing properties of physical objects during manipulation is technically challenging, thus making it difficult to study grip adaptation to variable dynamics or more complex object properties, e.g., with viscoelastic behavior. Most importantly, these approaches do not provide the experimenter with precise control over the interaction dynamics of a given viscoelastic force condition within or across trials, thus limiting the extent to which interaction kinematics and dynamics can be accurately measured.

Robotic devices are a promising approach to addressing the aforementioned limitations, as they can render variable dynamic environments under computer control during physical human–robot interaction. They provide reproducible and well-controlled force or position perturbations while being able to precisely quantify the response of the human operator. A handful of commercial multipurpose haptic devices, such as the PHANTOM Desktop/Premium (Geomagic, USA), the Omega/Delta (Force Dimension, Switzerland), or the Freedom 6S (MPB Technologies, Canada), are commonly used for the investigation of haptic perception and manipulation in virtual reality environments [14]–[16]. Nevertheless, such multipurpose haptic

Manuscript received February 10, 2014; revised May 27, 2014; accepted June 29, 2014. Date of publication July 8, 2014; date of current version December 18, 2014. The work of O. Lambercy and R. Gassert was supported by the NCCR Neural Plasticity and Repair of the Swiss National Science Foundation, J.-C. Metzger by the ETH CHIRP1 Research Grant on Cortically-Driven Assistance Adaptation during Sensorimotor Training, and M. Santello by a Collaborative Research Grant BCS-1153034 from the National Science Foundation. *Asterisk indicates corresponding author.*

O. Lambercy and J.-C. Metzger are with the Department of Health Sciences and Technology, ETH Zurich, 8092 Zurich, Switzerland (e-mail: olambercy@ethz.ch; jemetzge@ethz.ch).

*R. Gassert is with the Department of Health Sciences and Technology, ETH Zurich, 8092 Zurich, Switzerland (e-mail: gassertr@ethz.ch).

M. Santello is with the School of Biological and Health Systems Engineering, Arizona State university, Tempe, AZ 85004 USA (e-mail: marco.santello@asu.edu).

Color versions of one or more of the figures in this paper are available online at http://ieeexplore.ieee.org.

Digital Object Identifier 10.1109/TBME.2014.2336095

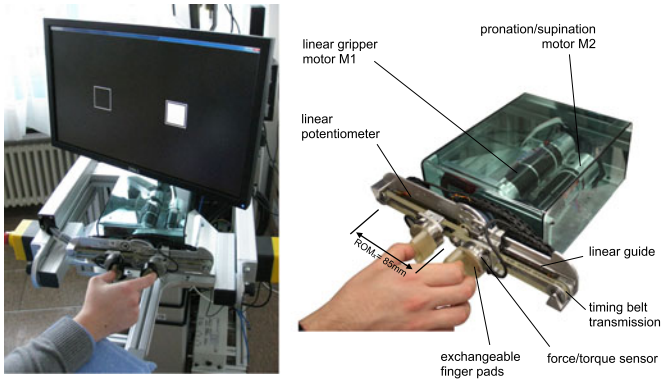

Fig. 1. (Left) overview of the robotic gripper and experimental setup. (Right) detailed view of the robot presenting the main components of the linear gripper. Motor M1 actuates the linear gripper, moving the two mechanically coupled finger pads over a belt transmission. The range of motion of the linear gripper ROM_x corresponds to a grasp aperture of 30–200 mm. Motor M2 actuates the rotation of the linear gripper over a range of 318° (not used in this study and locked by a brake).

devices are limited in the extent to which they can be used to investigate grasping dynamics and interaction with virtual objects of different viscoelastic properties. Specifically, the kinematics of most of these devices are optimized for 3-D arm movements rather than small finger movements, and present low structural stiffness. Furthermore, the continuous force (typically below 15 N) that common haptic devices can render limits the range of virtual mechanical properties that can be stably rendered. These limitations have motivated researchers to develop custom-made robotic setups dedicated to the study of grasping [17]–[20]. In particular, Tan and colleagues performed pioneering work using an electromechanically driven linear grasper to simulate different dynamic force fields at the index fingertip of healthy subjects [21]–[23]. The Planar Grasper proposed by Srinivasan and colleagues extended this approach by introducing independently controllable finger motion, and the option of simulating different force fields at each finger during precision grip [24]. These devices were used to determine human perceptual resolution or thresholds of force, compliance, viscosity, and mass, and investigate how these are influenced by visual feedback.

To the best of our knowledge, to date no study has focused on robotically modulating the interaction dynamics during a precision grasp-and-release task to investigate grasp control of variable virtual mechanical properties, nor grasp adaptation over time. This may be attributed to the lack of robotic devices capable of stably rendering a high range of interaction dynamics while precisely monitoring grip aperture and finger forces. Furthermore, in many of the prior studies involving robotic grippers, measurement of interaction kinematics and dynamics may have been affected by the mechanical impedance of the device, as these typically render virtual dynamics in open-loop impedance control.

In this paper, we propose a method to investigate how healthy human subjects adapt their precision grip force during dynamic interactions with viscoelastic force fields rendered by a single degree-of-freedom (DOF) robotic linear gripper with high dynamic range of achievable impedances, and pursue three objectives. The first objective is to demonstrate the ability of the robot to render different viscoelastic properties in a transparent, well-controlled, and reproducible manner, i.e., without the inherent dynamics of the robot affecting the interaction dynamics. The second objective is to verify the extent to which grasping force patterns elicited by the device correspond to force patterns associated with the grasping of freely held physical objects, for which subjects have to exert equal and opposite thumb and index grip forces, despite the mechanical coupling between the two finger pads. Finally, the third objective is to present proof-of-concept data from healthy subjects performing a grasp, hold, and release task with virtual objects of different combinations of stiffness and damping. We hypothesize that varying stiffness and/or damping will influence the rate and extent to which subjects adapt grip force to successfully perform a precision grasp-and-release task.

II. Materials and Methods

A. Apparatus

In the experiments described in this study, we used the *ReHapticKnob*, a robotic linear gripper that can generate high continuous forces and display a wide range of output impedances with high fidelity [25], [26] (see Fig. 1). Two adjustable finger pads mounted on two linear guides fixed to aluminum plates compose the linear gripper. Each finger pad is connected to the shaft of a motor-gear combination (M1, Re40, 150 W, and GP 42 C, Maxon Motor AG, Switzerland) through timing belts. As both finger pads are mechanically coupled, the movement of the fingers on the linear gripper is symmetrical, even if forces exerted by the thumb and index finger are different, or not in synchrony. Half cylinders made from rapid prototyping material (FullCure720) are used as finger pads, with a guiding groove into which the index finger and thumb can be inserted and fixed with Velcro straps. This ensures controlled and repeatable finger placement on the device, and offers the possibility to perform both grasping and releasing movements under load with the fingers in good contact with the device. A 6-DOF force/torque sensor (mini40, ATI Industrial Automation, USA) is mounted under each of the two finger pads to measure the interaction forces and torques, and is also used for the interaction control (impedance control with force feedback to compensate for the device dynamics [26], leading to a residual static friction $<$1.5 N). The position of the finger pads is measured through encoders (HEDL 5540, 2000 counts per turn, Avago, USA) mounted on the motor shaft. In addition, two linear potentiometers fixed along the linear guides provide redundant position sensing for initialization and safety. Encoder, potentiometer, and force sensor signals are acquired with two data acquisition cards (NI PCIe 6321 and NI PCI 6254, National Instruments, USA) on a real-time desktop computer (Intel Core 2 Quad 2.83 GHz, 2.0 GB RAM) running LabVIEW Real-Time 10.0 (National Instruments, USA) with a control loop at 1 kHz. Motor commands are sent to a DC servoamplifier (ADS 50/10 in current mode, Maxon Motor AG, Switzerland) that drives

TABLE I
RELEVANT PERFORMANCE CHARACTERISTICS OF THE LINEAR GRIPPER [25], [26]

range of motion	linear guide range: 85 mm finger aperture: 30-200 mm
position resolution	0.0024 mm/count
peak velocity	520 mm/s
peak acceleration	13.25 m/s^2
continuous force	88 N
peak force	1181 N
grip force sensing	range: $\pm$80 N resolution: 0.02 N
static friction	noncompensated: 6 N compensated: $<$ 1.5 N
compensated apparent mass	0.8 kg
closed-loop position bandwidth	6.6 Hz
closed-loop force bandwidth	9.3 Hz

TABLE II
COMBINATIONS OF STIFFNESS *K* AND DAMPING *B* OF THE VISCOELASTIC FORCE FIELDS PRESENTED TO SUBJECTS

Condition	Stiffness K	Damping B
C1	0 N/mm	0.02 Ns/mm
C2	0.25 N/mm	0.02 Ns/mm
C3	0.5 N/mm	0.02 Ns/mm
C4*	1 N/mm	0.02 Ns/mm
C5	0.5 N/mm	0 Ns/mm
C6	0.5 N/mm	0.05 Ns/mm
C7*	0.5 N/mm	0.1 Ns/mm
C8	0.5 N/mm	0.2 Ns/mm

*conditions performed by all eight subjects.

the motor of the linear gripper. Continuous forces of up to 88 N in both opening and closing directions can be generated. Mechanical end stops are placed to limit the range of the linear gripper (i.e., grip aperture) from 30 to 200 mm. The linear gripper unit is mounted on ball bearings, and a second motor-gear combination (M2, Re35, 90 W, and GP 32 HP, Maxon Motor AG, Switzerland) actuates its rotation over a timing belt. This second DOF is mechanically decoupled from the linear gripper. This rotational DOF was not used in this study, and was locked with a magnetic brake during all experiments, holding the linear gripper in a horizontal position. Table I summarizes the main properties of the haptic device used in these experiments. For a more detailed description of the mechanical design and control scheme, refer to [25] and [26].

B. Rendering of 1-DOF Viscoelastic Force Fields

Force fields of different viscoelastic properties were implemented as spring-damper components of different stiffness *K* and damping *B*, which are active from a specific contact point (i.e., force field boundary) x_0 in the range of motion of the linear gripper. The force *F* experienced by the user when in contact with the virtual object is given by

$$F(x,\dot{x}) = \begin{cases} K(x-x_0) + B\dot{x} & , \quad x > x_0 \\ 0 & , \quad x \leq x_0 \end{cases} \tag{1}$$

with F being the force generated at each finger pad of the linear gripper, x the actual position, and $\dot{x}$ the velocity of the finger pad along the axis defined by the linear gripper.

Eight viscoelastic parameter combinations were implemented and evaluated for the experiments described herein (see Table II). In the first four conditions (C1–C4), the stiffness *K* was modulated and the damping *B* remained constant, while in the last four conditions (C5–C8), the damping was varied while keeping the same stiffness. This choice of parameters was motivated by the goal of separately investigating the effect of modulating compliance or viscosity of the resisting force, which can hardly be achieved in an accurate and reproducible manner using instrumented physical objects. The proposed range of stiffness and damping coefficients was empirically chosen within the range that can be rendered by the robotic gripper in a stable way [26], and considering the human compliance and viscosity resolution [21], [23] to render virtual mechanical properties that subjects would be able to distinguish. Additional considerations were that a maximal force of 20 N to be applied by each finger (40 N reflected on the motor shaft) should prevent fatigue during repeated interactions with the rendered force field.

C. Grasp, Hold, and Release Task

A task consisting of three different phases, 1) *grasp*, 2) *hold*, and 3) *release*, was implemented on the robotic gripper to explore sensorimotor control during grasping in force fields of different viscoelastic properties. During the entire task, the robotic gripper simulated one of the combinations of stiffness and damping presented in Table II.

Grasp: This phase required controlling the linear horizontal movement of a cursor represented by a square box [40 mm $\times$ 40 mm; see Fig. 2(b)] displayed on a monitor placed in front of the subject. The cursor had to be moved from a start position, represented by a white rectangle (50 mm $\times$ 50 mm) on the right side of the screen, to a target position, represented by another white rectangle on the left side of the screen, by pinching the finger pads of the robotic gripper with the thumb and index finger. The cursor movement was scaled to correspond to a 20-mm movement of each of the finger pads, starting from a grip aperture of 85 mm. These values were selected based on the literature to ensure a grip aperture suitable for most participants during each phase of the task [27], [28]. The movement of the finger pads was kept constant for each condition, requiring subjects to produce varying force levels over a constant distance. For example, with a stiffness $K = 1$ N/mm, a force of 20 N was required for each finger to maintain the cursor on the target, while for a stiffness $K = 0.5$ N/mm, a force of only 10 N was required for each finger. A time window of 500 $\pm$ 100 ms was allowed to successfully move the cursor within a $\pm$1 mm error tolerance window. The time constraint required subjects to perform fast movements, and thus, to rely primarily on feedforward control to successfully achieve the task [3]. Indications for the timing of the task were provided through visual (red blinking indicator) and auditory cues (i.e., two preparation beeps followed by a 500-ms execution beep aligned with the successful

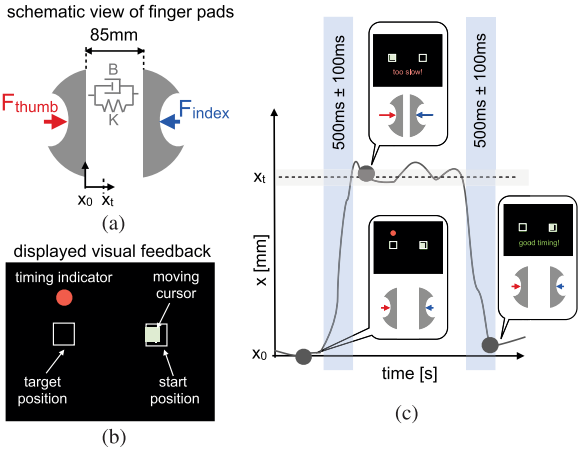

Fig. 2. Grasp, hold, and release task. (a) subjects were asked to grasp, hold, and release the linear gripper using their thumb and index finger in opposition (precision grip). The gripper rendered a viscoelastic force field, modeled as a spring-damper element of stiffness *K* and damping B. The grasp task consisted in a 20-mm movement of each finger pad (the movement of the two pads is mechanically coupled), from the rest position x_0 (85-mm grip aperture), where the subject entered the force field, to the target position x_t. (b) visual feedback on the task was given to the subject by means of two white boxes representing x_0 and x_t and a horizontally moving cursor displayed on a monitor. (c) a time constraint of 500 $\pm$ 100 ms was given for the grasp and release movements, whereas the duration of the hold phase was 3 s. Indications on the timing were provided through audio beeps and a blinking timing indicator displayed on the monitor above the target box. After the completion of each grasp or release movement, feedback about the timing (i.e., *too fast!*, *too slow!*, or *good timing!*) was provided.

completion time window). After the completion of each grasp trial, a feedback on the timing (e.g., *too fast!*, *too slow!*, or *good timing!*) was displayed on the monitor to motivate subjects and encourage learning of the task (see Fig. 2).

Hold: After reaching the target window, subjects were asked to hold the position for 3 s (indicated by auditory cues), and maintain the applied force. This duration was chosen to allow for enough time for subjects to stabilize the grip on the target before the onset of the release phase, while keeping the duration of force application short in order to prevent fatigue.

Release: The grasp force applied against the viscoelastic resisting force was released, which corresponded to a movement of the cursor back to its start position (represented by the white rectangle on the right side of the screen). Subjects were thus required to control the motion of the robot as the elastic energy stored in the virtual spring-damper element during the hold phase was released. As for the grasp phase, a time constraint (500 $\pm$ 100 ms) and a precision constraint ($\pm$1 mm error tolerance on the position to reach) were given for successful task completion. Similarly, indications for the timing of the task were given through visual and auditory cues, and timing feedback was displayed after the completion of the movement (terminal feedback).

One task trial corresponded to the execution of the three phases described previously. After the completion of a trial, a 3-s rest period was given during which subjects did not apply any grip force on the finger pads. At the end of this rest period, the auditory cues indicating the start of the grasp phase of the next trial were presented.

D. Pilot Study

Eight subjects (S1–S8, six males and two females, 34.6 $\pm$ 3.7 years old (mean$\pm$SE), six right- and two left handed) participated in a pilot experiment in which they were presented with four pseudo-randomly selected conditions among the ones described in Table II. Subjects could not anticipate the characteristics of the upcoming viscoelastic force field on the first trial of each block, but were instructed that these characteristics would remain the same across the entire block of trials. To allow for group data analysis, all subjects practiced in conditions C4 and C7. This choice was motivated by the desire to have one representative condition dominated by a high stiffness component (i.e., C4) and one representative condition dominated by a high damping component (i.e., C7). The other two conditions were pseudo-randomly selected from the eight parameters combinations. For each condition, subjects performed blocks of 30 consecutive trials to investigate grasp force adaptation during repeated dynamic interactions with each force field. The movement amplitude and the size of the target were kept fixed across all experimental conditions. Before the task, subjects were instructed on the conditions for a successful grasp, respectively, release (i.e., meeting both spatial and temporal constraints), but no instructions on how to modulate grip force during the task were provided. A 2-min break was given following each condition. The total duration of an experimental session was about 20 min.

For the entirety of the experiment, subjects sat on a chair positioned on the side of the robotic gripper, with their forearm resting on an adjustable padded support. The support was oriented with a 30° angle with respect to the robot to ensure a neutral wrist posture (i.e., in line with the forearm) when placing the fingers on the gripper (see Fig. 1). The height of the robotic gripper was adjusted to the subject to allow for a comfortable posture, via an actuated vertical column. This column fixes the vertical position of the gripper and supports its weight so that no load force (i.e., orthogonal to the grip) is required during precision grip. The thumb and index finger of the subjects dominant hand were fixed to the finger pads using Velcro straps. The experimental procedures were in accordance with the Declaration of Helsinki and approved by the ethics commission of the ETH Zurich (EK-2012-N-28). Subjects gave their written informed consent before performing the experiment.

E. Data Analysis

During the entire task, the normal interaction forces between the thumb/index finger and the respective finger pad (F_{thumb} and F_{index}, respectively) as well as forces and torques in other directions were recorded and stored for offline analysis. The position of the linear gripper was recorded simultaneously using the encoder signal. To simplify presentation of the results and given the mechanical coupling between the two finger pads, the x position is reported here as the movement of one of the finger supports with respect to the contact point with the force field boundary x_0, rather than as grip aperture (see Fig. 2). Velocity signals were differentiated from position data and

low-pass filtered using a second-order Butterworth filter with a cutoff frequency of 20 Hz. Force signals were also low-pass filtered using a second-order Butterworth filter with a cutoff frequency of 20 Hz.

1) Validation of Viscoelastic Force Field Rendering: For the purpose of validating the quality of the dynamic interaction with the viscoelastic force fields simulated by the robotic gripper, the actual stiffness force F_k and damping force F_b experienced by the user during the grasp phase were estimated from (1) by subtracting the theoretical damping (2) or stiffness (3) component from the applied force F (mean of thumb and index normal forces), respectively.

$$F_k(x) = K_e(x - x_0) = F(x, \dot{x}) - B\dot{x} \tag{2}$$

$$F_b(\dot{x}) = B_e\dot{x} = F(x, \dot{x}) - K(x - x_0). \tag{3}$$

For each trial, a linear regression was performed to estimate the experienced stiffness K_e and damping B_e.

2) Estimation of Temporal Coupling Between Fingertip Forces: For a rigid or a compliant object, grip force equilibrium is established by ensuring that digit grip forces match and that they are temporally coupled [29]. As our haptic device is grounded to a table and the two graspable surfaces (finger pads) are mechanically coupled, this constraint of mechanical equilibrium is removed. Therefore, grasping in the rendered 1-DOF viscoelastic force field could theoretically be achieved even when only one digit pushes on one finger pad, or when forces exerted by thumb and index finger are not temporally coupled. These considerations motivated the quantification of the temporal coordination of grip forces to determine the extent to which our device could replicate the physiological force coordination pattern observed during grasping of physical objects. Cross-correlations between the rate of thumb normal force and the rate of index finger normal force, i.e., the first time derivative of the normal forces, were computed. Force rates were preferred to forces to obtain a more sensitive measure of the phase relation between the two force signals and account for their nonstationarity [17]. Time lags between signals were varied from -100 to 100 ms, and the phase lag at which the correlation is maximal was calculated.

3) Adaptation to Viscoelastic Force Fields: To further quantify grasping performance and learning, the time required to complete the grasp was computed. Task dynamics were evaluated by measuring peak velocity and time to peak velocity during the grasp. Note that the analysis on adaptation presented in this paper focuses on the grasping phase of the task only, as this is–behaviorally–the most relevant aspect of the adaptation to a viscoelastic force field. The primary aim of this study is to present proof-of-concept data on the quality of the interaction with the robotic gripper, and how the grasp dynamics are influenced by different mechanical properties. The detailed analysis of adaptation during the hold and release phases, and how it is influenced by the performance in the grasp phase are beyond the scope of this paper and will be the focus of subsequent work with a larger pool of subjects.

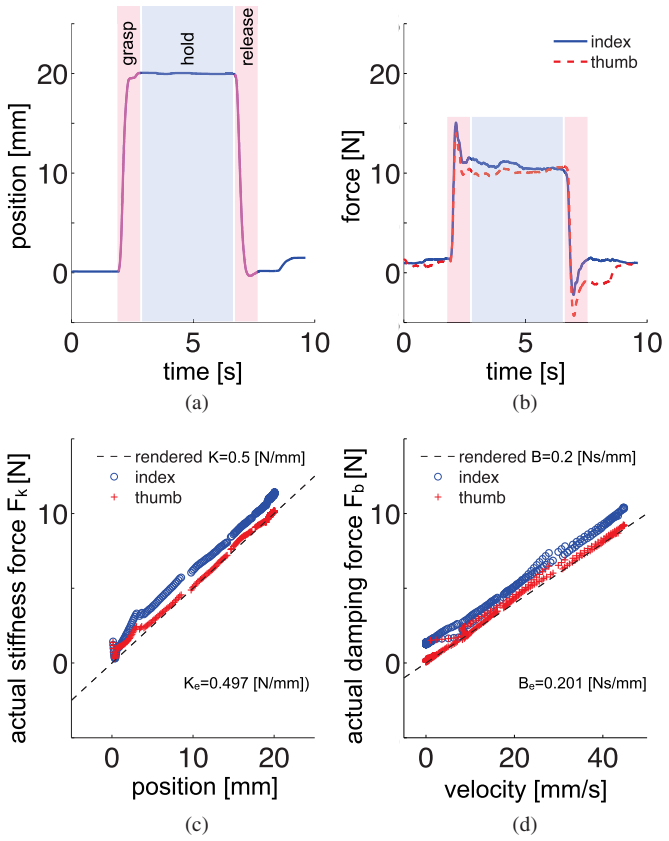

Fig. 3. (a) Position and (b) force data during one representative trial of subject S1 in condition C8. Grasp, hold and release phases are indicated by the shaded areas. In condition C8, the virtual spring-damper element has a stiffness of $K = 0.5$ N/mm and a viscosity of $B = 0.2$ Ns/mm. (c) and (d) represent the actual stiffness (F_k) and damping (F_b) experienced by the subject during interaction with the rendered force field, respectively. Dashed lines represent the modeled stiffness and damping of the viscoelastic force field, respectively.

III. Results

A. Validation of the Rendered Viscoelastic Force Fields

All subjects were able to complete the grasp, hold and release task. Position and normal force data in the three phases of a typical trial performed by one representative subject are shown in Fig. 3(a) and (b). As expected, the normal forces applied by the thumb and the index fingers are similar in amplitude and well coordinated during the grasp, hold, and release phases, despite the mechanical coupling between the two finger pads. This behavior was observed in more than 90% of the trials for all subjects. Horizontal and vertical tangential forces were also recorded and were found to be typically below 2 N, as the motion was purely along the grasping axis. To examine the interaction dynamics with the viscoelastic force field, stiffness (F_k), and damping (F_b) components of the grasp force applied by each finger during the grasp phase of the task were calculated [see Fig. 3(c) and (d)]. The stiffness and damping experienced by the user corresponded well to the desired viscoelastic properties of the rendered force field, with $K_e = 0.497$ N/mm and $B_e = 0.201$ Ns/mm, i.e., they were not altered by the apparent dynamics of the haptic device, which were well compensated by the impedance control with force

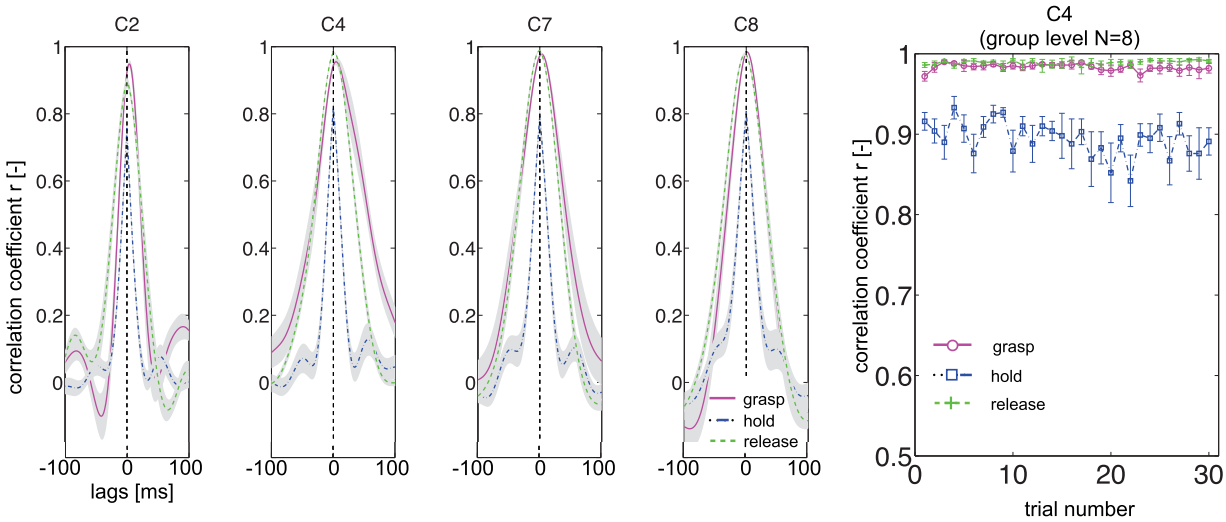

r [-]	C2	C4	C7	C8
grasp	0.959	0.963	0.981	0.986
hold	0.757	0.820	0.794	0.807
release	0.903	0.984	0.989	0.982

Fig. 4. Left: cross correlations of thumb normal force rate and index finger normal force rate during grasp, hold, and release phases, averaged across all trials (mean ± 95% confidence interval) for each of the experimental conditions (C2, C4, C7, C8) of one representative subject (S1). The cross-correlation coefficients at 0 s lag of all phases (r) are reported in the table. Right: evolution of cross-correlation coefficients over the 30 trials of condition C4 for the three phases of the grasp and release task (mean over the eight subjects ± SE).

feedback scheme. Over all conditions and subjects, the average discrepancies between desired stiffness (damping) and the experienced stiffness (damping) were 0.039 N/mm (0.004 Ns/mm). The hysteresis of the robot rendered force fields during grasp and release of the end-effector was investigated separately by successively performing grasp and release movements in the representative conditions C1, C3, C5, and C8. Hysteresis was found to be below 2 N in all conditions, therefore not affecting the impedance rendering perceived in the different phases of the task.

B. Temporal Coordination of Digit Forces

The cross-correlation coefficients of force rates during grasp, hold, and release phases, averaged across all 30 trials (mean±95% confidence interval) and for the four experimental conditions (C2, C4, C7, C8) performed by one representative subject are shown in Fig. 4. A high correlation between rates of normal forces was found for all phases of the task during which the subject actively applied force against the viscoelastic force field. The average lag at which the correlation was maximal ranged between −2.3 and 5.9 ms in all conditions for this subject. A similar behavior was observed for all other subjects and experimental conditions, with an average (SE) correlation of 0.958 (0.016) for the grasp phase, 0.821 (0.016) for the hold phase and 0.956 (0.014) for the release phase, and average lags ranging from −10.0 to 6.3 ms. Moreover, the high level of coordination between index finger and thumb was maintained over the entire sequence of 30 trials of a condition (see Fig. 4). These data indicate that subjects actively used both fingertips in a coordinated fashion to generate forces on the finger pads and move them against the different viscoelastic force fields. Furthermore, the difference in magnitude between index and thumb forces remained small over all conditions and subjects, with an average (SE) difference of 2.02 N (0.26 N).

C. Adaptation to Viscoelastic Dynamics During Precision Grip

Subjects were able to complete the grasp-and-release task under each condition rendered by the robotic gripper, reaching the target within the temporal and spatial constraints after a few trials. Fig. 5(a) shows the learning curves computed over the 30 trials averaged across all subjects for the two experimental conditions performed by all eight subjects (C4 and C7). In both conditions, subjects performed poorly in the first trial, with an average (SE) movement duration of 1496 ms (169 ms) for C4, and 1355 ms (329 ms) for C7. This was expected as this initial trial corresponded to the first exposure to the unknown viscoelastic properties. In condition C4, subjects required about seven trials to successfully reach the target and perform the grasping movement within the time constraint (represented by the shaded area). In condition C7, subjects were able to successfully perform the task on their second trial. Furthermore, the within-subject performance variability was marginally smaller in condition C7 (paired t-test, $p = 0.057$).

Fig. 5(b) shows the time course of grasp velocity profiles averaged over groups of five trials for one representative subject (S1) for conditions C4 and C7 to illustrate how this subject

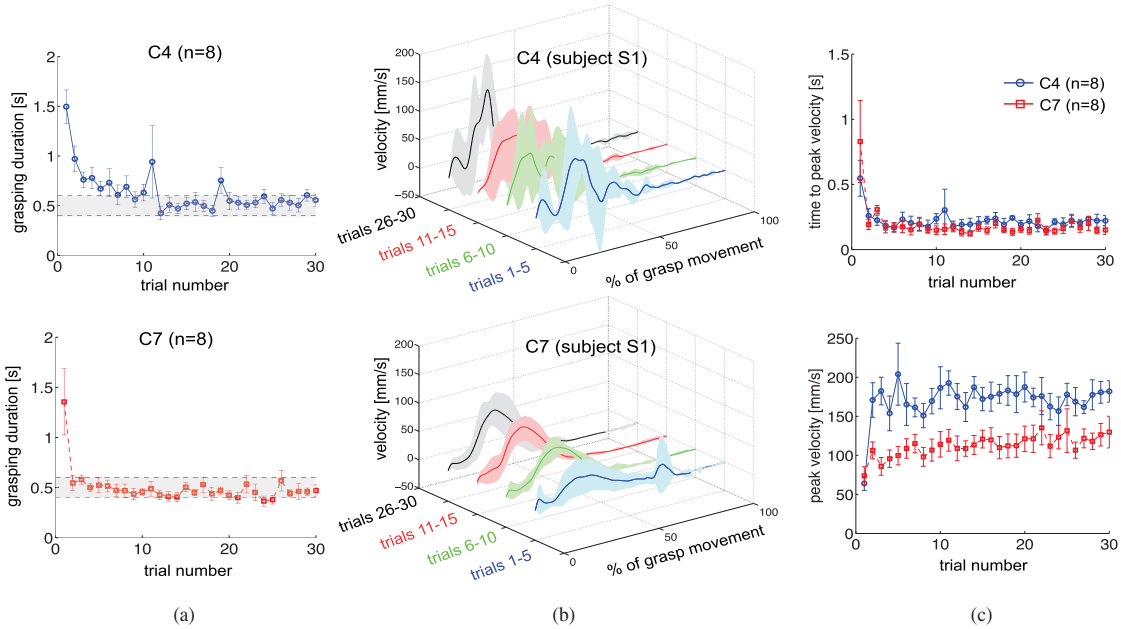

Fig. 5. (a) mean±SE over the eight subjects of the grasp duration, i.e., the time to reach the target position x_t, for condition C4 (top) and condition C7 (bottom). Shaded areas represent the time constraint of 500 ± 100 ms for the movement to be considered successful. (b) evolution of the velocity profile during grasping movements for conditions C4 (top) and C7 (bottom) of one representative subject (S1). Velocity profiles were first normalized over the movement duration, and then averaged over groups of five trials. The mean velocity with 95% confidence intervals is presented for each block of trials. (c) evolution of time to peak velocity (top) and amplitude of peak velocity (bottom) for conditions C4 and C7 (mean±SE for the eight subjects).

adapted to different task dynamics. In the first group of trials of interaction with a high stiffness and low damping force field (C4), multiple velocity peaks can be observed, with a gradual decrease over the subsequent trials. Due to the high rendered stiffness, the robotic gripper generated a large resistance during motion, and a large rate of change of resistance, which in the absence of damping led to a more unstable grasp. In the case of a higher damping force field (C7), oscillations in the velocity profiles are reduced, even for the initial trials. To further illustrate differences in grasp dynamics caused by different viscoelastic properties, Fig. 5(c) presents group data for the timing and amplitude of the velocity peak of the grasp movement. Interestingly, despite the different viscoelastic force field properties, the timing of the velocity peak is similar among both conditions. With the exception of the first trial, during which subjects were exposed to the force field dynamics for the first time, they quickly adapted their grasp to produce peak velocity around 150 ms after the onset of movement. Conversely, the amplitude of the peak velocity shows a different behavior for each condition. In condition C7, peak velocity remained small in all subjects due to the higher damping. In condition C4, the learning of the task was associated with a progressive increase in peak velocity.

IV. Discussion

A. Validation and Methodological Considerations

In this paper, we presented a novel method to investigate the dynamic control of two-digit grasping under well-controlled and reproducible conditions. We report on validation analyses and proof-of-concept data from a grasp, hold, and release task involving interactions with different 1-DOF viscoelastic force fields. The main results of this study are consistent with findings from previous studies that investigated grasping of compliant physical objects [9]. During grasping, holding, and releasing within the viscoelastic force fields, normal forces applied by the thumb and index finger were similar in amplitude and characterized by a high degree of temporal coordination (see Fig. 4). This behavior is expected from interaction with rigid objects during precision grip. However, when using our robotic gripper, the movement of the fingers is mechanically coupled when subjects grasp within the resistive viscoelastic force field, i.e., the task could have been accomplished by using only one finger to press against the respective finger pad. Nevertheless, cross-correlation analysis showed a high correlation between the rates of thumb and index finger forces during the grasp, hold, and release phases of the task, and lags between these signals were found to be below 10 ms across all trials and subjects. These data demonstrate that subjects exerted forces and generated motion in a coordinated fashion with thumb and index finger while interacting with the robotic gripper and that, despite the additional constraint introduced by the mechanical coupling of the pads, subjects performed the grasp in a physiological fashion. Correlation coefficients were found to be stable over 30 trials of a condition, further indicating that subjects did not progressively modify their grip pattern to take advantage of the mechanical coupling of the finger pads. This validates the single DOF robotic linear gripper and the proposed method as a suitable tool to study precision grip control.

B. Adaptation of Grasp Control to Virtual Object Viscoelastic Properties

All subjects were able to perform the grasp-and-release task for each experimental condition. Subjects typically learned the force field dynamics and generated suitable patterns of grasping forces within the first seven trials (see Fig. 5). These results are in agreement with previous studies using real objects with unpredictable mechanical properties, showing that only few trials are needed for the adaptation of digit force distribution [10], [30]. An analysis of the trial-to-trial evolution of velocity profiles revealed that subjects adapted their motor behavior differently depending on the viscoelastic properties of the force field. In all conditions, a progressive blending of grasp submovements could be observed, thus confirming that, over trials, subjects learned to perform the task in a smoother way (reduction in the number of velocity peaks), requiring less corrective actions [31], [32]. The time course of force development during the grasping phase was similar among all conditions and this finding is consistent with the results of Winges and colleagues who found no change in grip force temporal coordination pattern during three-digit grasping of objects with variable compliance [9]. Nevertheless, peak grasp velocity differed across conditions. In the task conditions investigated herein, force fields with high stiffness and low damping (e.g., C4) allowed for fast movements, but required corrective actions to stabilize oscillations. In the initial trials, multiple velocity peaks could be observed. This profile is considered indicative of feedback-driven corrective force modulation during initial interaction with the unknown force field. This behavior progressively disappeared over trials, giving way to mostly one main bell-shaped velocity peak of higher amplitude, a phenomenon normally associated with anticipatory (feed-forward) force modulation [2]. Force fields with higher viscosity (e.g., C7), although limiting peak velocity, provided more stability when applying fast positional changes, which resulted in fewer oscillations during the grasping. These two behaviors might well result from the selection of different control strategies modulated as a function of the perceived object properties and might reflect different levels of difficulty experienced by the subject. The differences in task difficulty could be due to a more efficient coupling between the impedance rendered by the robot and the impendance of the human hand (as reported in [12] and [32]–[35]) in conditions where the rendered stiffness is low (overdamped system (C7) versus underdamped system (C4)). These observations should nevertheless be taken with caution, as the present proof-of-concept study was limited by a relatively small number of participants, and by only two conditions that were performed by all participants. The adaptation to different viscoelastic forces itself needs to be investigated in more depth and will be the object of future work, e.g., to explore which parameter combinations maximally challenge subjects during sensorimotor adaptation to object viscoelastic properties.

The proposed robotic approach to investigate precision grip control offers several advantages. First, mechanical properties of the force fields rendered by the robotic gripper can be modified without any visually perceivable changes to the setup, on a condition or even trial-by-trial basis. It is well known that subjects can associate visual object cues such as size or shape to the weight or mass distribution of the object, and that these cues play an important role in the anticipatory control of digit forces for grasping [8], [36]–[38]. Being able to vary properties of an object to be grasped without changing the visual appearance is thus crucial to the investigation of sensorimotor adaptation mechanisms to mechanical object properties. Second, the performance of the robotic gripper offers the possibility to render a wide range of virtual mechanical properties, such as more complex or unnatural force fields, as any parameter combination within the tested values and even beyond (e.g., negative damping) could theoretically be rendered by the system. The linear gripper is capable of generating continuous forces over 80 N, has low residual friction (below 1.5 N, thanks to impedance control with force feedback), and a force control bandwidth of about 9 Hz [26], which is greater than that of voluntary human finger movement [39]. Furthermore, the end-effector-based design of the linear gripper with exchangeable finger pads allows to cope with a wide range of grip spans ranging from 30 to 200 mm, making it versatile and easily adaptable to different hand sizes and shape. These characteristics go beyond what is currently possible with most commercially available haptic devices, or robotic linear grippers designed to provide short force or position perturbations. Finally, the ability of the robot to precisely quantify fingertip forces, both along and transverse to the direction of movement, as well as grasp aperture during interaction with viscoelastic force fields, promises a novel method to investigate the transition between motion and force generation during object grasping [40]. As limitations of the linear gripper, we should underline that the gripper is fixed in the vertical direction, therefore, not allowing the investigation of grip/load coupling during grasping and lifting of virtual objects.

C. Potential Implications for the Study of Sensorimotor Control of Grasping and Rehabilitation of Hand Function

The proof of principle presented in this paper demonstrated that a linear gripper with two mechanically coupled moveable finger pads (i.e., 1 DOF) is an adequate model to study physiological precision grip. In the field of biomechanical engineering, this impacts design guidelines for rehabilitation devices, neuroscience tools, or biomedical instruments interacting with the human through precision grip, potentially leading to the development of simpler devices.

Our study further underscores the potential of a robotic approach to investigate precision grip control and opens several research avenues. The proposed method provides a novel tool to investigate grip force adaptation mechanisms to various force fields, and has the potential to provide novel insights on how object mechanical properties are perceived, encoded/updated, and retrieved during explorative object interaction, allowing to test theoretical frameworks of motor control and learning. Applied to neurologically impaired subjects, the developed method bears multiple promises. Impairment in precision grip force control during manipulation of rigid objects is well documented

[41]–[44], but it has been less studied in the case of nonrigid objects. The proposed method will allow to investigate whether a 1-D linear gripper can assess pathological behavior during precision grip (e.g., improper finger force coordination, force modulation and force direction). Furthermore, it will give insights on whether the ability to adapt to unknown precision grip dynamics is impaired in neurological patients, by quantifying the evolution of behavioral readings. This has the potential to influence the design of novel hand rehabilitation platforms, as well as the implementation of rehabilitation exercises focusing on precision grip, to render loads with specific viscoelastic properties to challenge neurological patients.

ACKNOWLEDGMENT

The authors would like to thank W. Popp for his help with the acquisition of pilot data, and all the subjects who participated in the study.

REFERENCES

[1] J. Flanagan, M. Bowman, and R. Johansson, "Control strategies in object manipulation tasks," *Current Opinion Neurobiol.*, vol. 16, no. 6, pp. 650–659, 2006.

[2] R. Johansson and K. Cole, "Sensory-motor coordination during grasping and manipulative actions," *Current Opinion Neurobiol.*, vol. 2, no. 6, pp. 815–823, 1992.

[3] R. Johansson and R. Flanagan, "Coding and use of tactile signals from the fingertips in object manipulation tasks," *Nat. Rev. Neurosci.*, vol. 10, no. 5, pp. 345–359, 2009.

[4] R. Johansson and G. Westling, "Coordinated isometric muscle commands adequately and erroneously programmed for the weight during lifting task with precision grip," *Exp. Brain Res.*, vol. 71, no. 1, pp. 59–71, 1988.

[5] G. Westling and R. Johansson, "Factors influencing the force control during precision grip," *Exp. Brain Res.*, vol. 53, no. 2, pp. 277–284, 1984.

[6] K. Cole and R. Johansson, "Friction at the digit-object interface scales the sensorimotor transformation for grip responses to pulling loads," *Exp. Brain Res.*, vol. 95, no. 3, pp. 523–532, 1993.

[7] R. Johansson and G. Westling, "Roles of glabrous skin receptors and sensorimotor memory in automatic control of precision grip when lifting rougher or more slippery objects," *Exp. Brain Res.*, vol. 56, no. 3, pp. 550–564, 1984.

[8] I. Salimi, I. Hollender, W. Frazier, and A. Gordon, "Specificity of internal representations underlying grasping," *J. Neurophysiol.*, vol. 84, pp. 2390–2397, 2000.

[9] S. Winges, S. Eonta, J. Soechting, and M. Flanders, "Effects of object compliance on three-digit grasping," *J. Neurophysiol.*, vol. 101, pp. 2447–2458, 2009.

[10] W. Zhang, A. Gordon, T. McIsaac, and M. Santello, "Within-trial modulation of multi-digit forces to friction," *Exp. Brain Res.*, vol. 211, no. 1, pp. 17–26, 2011.

[11] F. Valero-Cuevas, N. Smaby, M. Venkadesan, M. Peterson, and T. Wright, "The strength-dexterity test as a measure of dynamic pinch performance," *J. Biomech.*, vol. 36, no. 2, pp. 265–270, 2003.

[12] C. Van Doren, "Differential effects of load stiffness on matching pinch force, finger span, and effort," *Exp. Brain Res.*, vol. 120, no. 4, pp. 487–495, 1998.

[13] M. Venkadesan, J. Guckenheimer, and F. Valero-Cuevas, "Manipulating the edge of instability," *J. Biomech.*, vol. 40, no. 8, pp. 1653–1661, 2007.

[14] M. Ernst and M. Banks, "Humans integrate visual and haptic information in a statistically optimal fashion," *Nature*, vol. 415, no. 6870, pp. 429–433, 2002.

[15] E. Weiss and M. Flanders, "Somatosensory comparison during haptic tracing," *Cerebral Cortex*, vol. 21, no. 2, pp. 425–434, 2011.

[16] R. Yokogawa and K. Hara, "Manipulabilities of the index finger and thumb in three tip-pinch postures," *J. Biomech. Eng.*, vol. 126, no. 2, pp. 212–219, 2004.

[17] J. Flanagan and A. Wing, "The role of internal models in motion planning and control: evidence from grip force adjustments during movements of hand-held loads," *J. Neurosci.*, vol. 17, pp. 1519–1528, 1997.

[18] J. Hermsdorfer, N. Mai, and C. Marquardt, "Evaluation of precision grip using pneumatically controlled loads," *J. Neurosci. Methods*, vol. 45, pp. 117–126, 1992.

[19] V. Zatsiorsky, F. Gao, and M. Latash, "Prehension stability: Experiments with expanding and contracting handle," *J. Neurophysiol.*, vol. 95, pp. 2513–2529, 2006.

[20] Y. Sun, J. Park, V. M. Zatsiorsky, and M. L. Latash, "Prehension synergies during smooth changes of the external torque," *Exp. Brain Res.*, vol. 213, no. 4, pp. 493–506, 2011.

[21] G. Beauregard, M. Srinivasan, and N. Durlach, "The manual resolution of viscosity and mass," in *Proc. ASME Dyn. Syst. Control Division*, vol. 1, 1995, pp. 657–662.

[22] H. Tan, X. Pang, and N. Durlach, "Manual resolution of length, force, and compliance," *Adv. Robot.*, vol. 42, pp. 13–18, 1992.

[23] H. Tan, N. Durlach, G. Beauregard, and M. Srinivasan, "Manual discrimination of compliance using active pinch grasp - the roles of force and work cues," *Perception Psychophys.*, vol. 57, no. 4, pp. 495–510, 1995.

[24] M. Srinivasan, G. Beauregard, and D. Brock, "The impact of visual information on the haptic perception of stiffness in virtual environments," in *Proc. ASME Dyn. Syst. Control Division*, 1996, pp. 555–559.

[25] J.-C. Metzger, O. Lambercy, D. Chapuis, and R. Gassert, "Design and characterization of the rehapticknob, a robot for assessment and therapy of hand function," in *Proc. IEEE/RSJ Int. Conf. Intell. Robots Syst.*, 2011, pp. 3074–3080.

[26] J.-C. Metzger, O. Lambercy, and R. Gassert, "High-fidelity rendering of virtual objects with the rehapticknob - novel avenues in robot-assisted rehabilitation of hand function," in *Proc IEEE Haptics Symp.*, 2012, pp. 51–56.

[27] W. Snapp-Childs, R. Coats, J. S. Pan, M. Mon-Williams, and G. P. Bingham, "Intrinsic scaling of reaches-to-grasp predicted by affordance-based model: Testing men and women with large and small grip spans," *J. Vision*, vol. 11, no. 11, pp. 973–973, 2011.

[28] J. R. Ruiz, V. España-Romero, F. B. Ortega, M. Sjöström, M. J. Castillo, and A. Gutierrez, "Hand span influences optimal grip span in male and female teenagers," *J. Hand Surg.*, vol. 31, no. 8, pp. 1367–1372, 2006.

[29] M. Santello and J. Soechting, "Force synergies for multifingered grasping," *Exp. Brain Res.*, vol. 133, no. 4, pp. 457–467, 2000.

[30] Q. Fu, W. Zhang, and M. Santello, "Anticipatory planning and control of grasp positions and forces for dexterous two-digit manipulation," *J. Neurosci.*, vol. 30, pp. 9117–9126, 2011.

[31] T. Flash and N. Hogan, "The coordination of arm movements: an experimentally confirmed mathematical model," *J. Neurosci.*, vol. 5, no. 7, pp. 1688–1703, 1985.

[32] T. Milner, "A model for the generation of movements requiring endpoint precision," *Neuroscience*, vol. 49, no. 2, pp. 487–496, 1992.

[33] R. Dong, J. Wu, T. McDowell, D. Welcome, and A. Schopper, "Distribution of mechanical impedance at the fingers and the palm of the human hand," *J. Biomech.*, vol. 38, no. 5, pp. 1165–1175, 2005.

[34] A. E. Fiorilla, F. Nori, L. Masia, and G. Sandini, "Finger impedance evaluation by means of hand exoskeleton," *Ann. Biomed. Eng.*, vol. 39, no. 12, pp. 2945–2954, 2011.

[35] A. Z. Hajian and R. D. Howe, "Identification of the mechanical impedance at the human finger tip," *J. Biomech. Eng.*, vol. 119, no. 1, pp. 109–114, 1997.

[36] Q. Fu and M. Santello, "Context-dependent learning interferes with visuomotor transformations for manipulation planning," *J. Neurosci.*, vol. 32, pp. 15 086–15 092, 2012.

[37] A. Gordon, H. Forssberg, R. Johansson, and G. Westling, "Visual size cues in the programming of manipulative forces during precision grip," *Exp. Brain Res.*, vol. 83, no. 3, pp. 477–482, 1991.

[38] L. Schettino, S. Adamovich, and H. Poizner, "Effects of object shape and visual feedback on hand configuration during grasping," *Exp. Brain Res.*, vol. 151, no. 2, pp. 158–166, 2003.

[39] W. Yu, S. Kilbreath, R. Fitzpatrick, and S. Gandevia, "Thumb and finger forces produced by motor units in the long flexor of the human thumb," *J. Physiol.*, vol. 583, pp. 1145–1154, 2007.

[40] M. Venkadesan and F. Valero-Cuevas, "Neural control of motion-to-force transitions with the fingertip," *J. Neurosci.*, vol. 28, no. 6, pp. 1366–1373, 2008.

[41] R. S. Johansson, C. Häger, and R. Riso, "Somatosensory control of precision grip during unpredictable pulling loads," *Exp. Brain Res.*, vol. 89, no. 1, pp. 192–203, 1992.

[42] D. A. Nowak and J. Hermsdörfer, "Grip force behavior during object manipulation in neurological disorders: toward an objective evaluation of manual performance deficits," *Movement Disorders*, vol. 20, no. 1, pp. 11–25, 2005.
[43] V. Iyengar, M. J. Santos, M. Ko, and A. S. Aruin, "Grip force control in individuals with multiple sclerosis," *Neurorehabilitation Neural Repair*, vol. 23, no. 8, pp. 855–861, 2009.
[44] W. Zhang, J. A. Johnston, M. A. Ross, A. A. Smith, B. J. Coakley, E. A. Gleason, A. C. Dueck, and M. Santello, "Effects of carpal tunnel syndrome on adaptation of multi-digit forces to object weight for whole-hand manipulation," *PloS one*, vol. 6, no. 11, p. e27715, 2011.

Olivier Lambercy (S'06–M'10) received the M.Sc. degree in microengineering from the Ecole Polytechnique Fédérale de Lausanne, Lausanne, Switzerland, in 2005 and the Ph.D. degree in mechanical engineering from the National University of Singapore, Singapore in 2009.

His main contributions are in the field of robot-assisted rehabilitation of hand function after stroke. During his thesis, he participated in the development and evaluation of some of the first robotic devices dedicated to hand rehabilitation in Singapore, Canada, and Switzerland. Since 2009, he has been a Research Associate at the Rehabilitation Engineering Lab, Swiss Federal Institute of Technology Zurich, Switzerland. His main research interests include medical and rehabilitation robotics, motor control and human–machine interaction.

Jean-Claude Metzger (S'11) received the B.Sc. and M.Sc. degrees in mechanical engineering (focus in robotics, systems, and control) from the Swiss Federal Institute of Technology Zurich (ETHZ), Switzerland, in 2006 and 2010, respectively, where he is currently working toward the Ph.D at the Rehabilitation Engineering Lab.

His research interests include the field of physical human–robot interaction and robot-assisted rehabilitation.

Marco Santello (M'12) received the Diploma degree in Educazione Fisica (equivalent to B.S. in kinesiology) from the University of L'Aquila, L'Aquila, Italy, in 1990 and the Ph.D. degree in sport and exercise sciences from the University of Birmingham, Birmingham, U.K., in 1995.

After his postdoctoral training at the Department of Physiology, University of Minnesota, Minneapolis, MN, USA (1995–1999), he has been a Faculty Member at the Department of Kinesiology (1999–2010) and the School of Biological and Health Systems Engineering (2010 to date) at Arizona State University, Tempe, AZ, USA. He is currently a Professor of biomedical engineering, the Director of the School of Biological and Health Systems Engineering, and Harrington Endowed Chair. His research interests include neural control of movement, sensorimotor learning, noninvasive brain stimulation, biological signal processing, rehabilitation robotics, and human–machine interactions. He is an Associate Editor of *Neuroscience and Biomedical Engineering*, and a Member of the Editorial Board of the IEEE TRANSACTIONS ON HAPTICS, SCIENTIFICA and the *Journal of Assistive, Rehabilitative and Therapeutic Technologies*.

Roger Gassert (S'02–M'06–SM'13) received the M.Sc. degree in microengineering and the Ph.D. degree in neuroscience robotics from the Ecole Polytechnique Fédérale de Lausanne, Lausanne, Switzerland, in 2002 and 2006, respectively.

Since 2008, he has been an Assistant Professor of rehabilitation engineering at the Swiss Federal Institute of Technology Zurich, Switzerland. He has made contributions to the field of neuroscience robotics to investigate sensorimotor control and related dysfunctions, as well as to robot-assisted assessment and therapy. His research interests include human–machine interaction, rehabilitation robotics, assistive technology, and the neural control of movement.